

Optical discrete solitons in waveguide arrays.

I. Soliton formation

H. S. Eisenberg, R. Morandotti,* and Y. Silberberg

Department of Physics of Complex Systems, Weizmann Institute of Science, Rehovot, Israel, 76100

J. M. Arnold and G. Pennelli

Department of Electronics and Electrical Engineering, University of Glasgow, Glasgow, Scotland, G12 8QQ

J. S. Aitchison*

The Edward S. Rogers Sr. Department of Electrical and Computer Engineering, University of Toronto, Toronto, Ontario, Canada M5S 3G4

Received October 31, 2001; revised manuscript received July 25, 2002

We investigate the generation of discrete spatial solitons in arrays of coupled waveguides. Light was launched into the center of the array, and different beam sizes and array geometries were tested. At low power, the propagating field spreads as it couples to more waveguides. When the intensity is increased, localization is observed around the input waveguides, leading to the formation of a discrete soliton. For wide input beams, exciting a few waveguides, soliton splitting, which is due to instability induced by multiphoton absorption, is observed. All of these effects are described well by a coupled-mode formalism. © 2002 Optical Society of America

OCIS codes: 190.5530, 190.3270, 230.7380.

1. INTRODUCTION

The study of optical solitary phenomena has been a constantly growing field for almost 30 years. Since Zakharov and Shabat formulated the basic theory for instantaneous Kerr solitons,¹ such solitons have been demonstrated in the time domain as well as in the space domain. In time, high-peak-power, short pulses of light in optical fibers were shown to avoid broadening by dispersion and retain their temporal shape.² In space an intense light beam was propagated inside a planar waveguide in which diffraction is possible in only one transverse direction, without a change in its profile occurring.^{3,4} Other optical soliton phenomena have been proposed and demonstrated. Some examples are quadratic solitons⁵ and photorefractive solitons.^{6,7} Another subject that has attracted considerable attention is nonlinear waves in discrete systems. When such waves are self-trapped, they are known as discrete solitons. They were predicted theoretically by Christodoulides and Joseph⁸ and recently observed experimentally.⁹

Nonlinear discrete systems are encountered in various fields of physics. They appear in different contexts and span a vast range of scales, yet share the common phenomenon of nonlinear wave localization. Among the examples, we list localized modes in molecular systems such as long proteins,¹⁰ polarons in one-dimensional ionic crystals,¹¹ localized modes in electrical lattices,¹² and coupled arrays of nonlinear mechanical pendulums.¹³ These localized modes are examples of the more general

phenomenon of discrete breathers¹⁴ to which discrete solitons belong. A number of other examples are reviewed in Ref. 14.

A simple optical discrete system is a set of coupled identical single-mode linear waveguides. During propagation, light energy is transferred among the waveguides through linear coupling. The linear coupling is the result of the spatial overlap of the individual waveguide modes. The broadening of light propagating in such an array is referred to as discrete diffraction. If we denote the scalar electrical field of the single mode of the n th waveguide as E_n , the infinite set of equations describing propagation in an infinite array of waveguides is⁸

$$i \frac{dE_n}{dz} + \beta E_n + C(E_{n-1} + E_{n+1}) + \gamma |E_n|^2 E_n = 0, \quad (1)$$

where β is the linear propagation constant, C is the coupling constant, $\gamma = \omega_0 n_2 / c A_{\text{eff}}$, ω_0 is the optical angular frequency, n_2 is the nonlinear coefficient, and A_{eff} is the common effective area of the waveguide modes. This equation is sometimes referred to as the discrete nonlinear Schrödinger equation. At low powers, the nonlinear term of Eq. (1) can be ignored. The infinite set of ordinary differential equations is then analytically integrable.¹⁵ The solution for the n th waveguide, when only one waveguide is excited, is a set of Bessel functions. If we set $E_0 = A_0$ and $E_{n \neq 0} = 0$ at $z = 0$, the solution for the electrical field in the n th waveguide is

$$E_n(z) = A_0 (i)^n \exp(i\beta z) \mathcal{I}_n(2Cz), \quad (2)$$

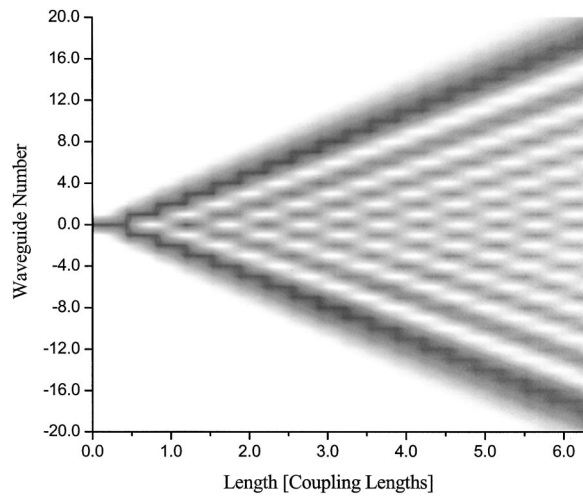


Fig. 1. Solution for a linearly coupled array of 41 waveguides, when light is injected into the central waveguide, with $E_0 = 1$. The intensity is shown in gray scale. The scale is chosen such that the peak intensity for every propagation distance along the waveguide is represented by black. The energy is spread mainly into two lobes. The number of central peaks is an indication to how many coupling lengths the light has propagated.

where $\mathcal{I}_n(x)$ is a Bessel function of order n . This evolution of the light distribution is displayed in Fig. 1. As the light propagates along the waveguides, the energy spreads into two main lobes with several secondary peaks between them. The solution under any other initial condition will be a linear superposition of Eq. (2). When the intensity varies slowly over adjacent waveguides, the discrete set of ordinary differential equations [Eq. (1)] can be reduced to the nonlinear Schrödinger equation that describes diffraction for weak continuous beams and spatial solitons for intense beams.⁸ It has been shown numerically^{8,16,17} that at high-enough power the introduction of a field distribution to the array such as $E_n(z) = A_0 \exp[i(2C + \beta)z] \text{sech}(X_n/X_0)$, where X_n is the location of the n th waveguide and X_0 is the characteristic width, will result in a localized propagating distribution.

This localized wave in a discrete system is known as a discrete soliton. It has been predicted to have a few properties shared with more familiar continuum solitons: A discrete soliton propagates without a change in its power distribution; a discrete soliton can propagate at an angle to the waveguide direction^{17,18}; two nearby discrete solitons apply forces on each other according to their relative phases¹⁷; and a discrete dark soliton solution also exists¹⁹ as well as vectorial confined solutions.²⁰ Nevertheless, there are many differences between continuum and discrete solitons that appear because of discreteness. Both translational and rotational symmetries are broken. Discreteness induces a generalized periodic potential for the light, known as the Peierls–Nabarro potential.²¹ The Peierls–Nabarro potential leads to two types of discrete soliton, one stable and the second unstable. The stable soliton is symmetrically set around a waveguide of the array, whereas the unstable one is centered around the midpoint between two waveguides (so that the two waveguides nearest to this center carry equal power). The Peierls–Nabarro potential affects the propagation in many ways. A high-power, angled discrete soliton can be

trapped in this potential, preventing it from traveling sideways in the array.¹⁷ This potential can also enhance small lateral deviations of the initial input.¹⁸ When two discrete solitons collide, the collision is inelastic, and they may merge together, unlike the case of two continuum solitons.¹⁷ Dark discrete solitons can be formed in a positive Kerr material, whereas continuum dark solitons cannot, because of the special properties of discrete diffraction.¹⁹ An effective potential can be introduced on discrete solitons when the homogeneity of the waveguide array is changed.^{22–25}

It is the purpose of this paper to describe in detail the experimental demonstration of self-trapping in a nonlinear array, extending the initial results reported in Ref. 9. This paper is organized as follows. In Section 2 the experimental setup and samples are described. The basic demonstration of an optical discrete soliton is presented in Section 3, and then we show the effects of the input beam shape on the discrete soliton formation in Section 4. Finally, conclusions are presented in Section 5. An accompanying paper,²⁶ will concentrate on experimental studies of the dynamical properties of these solitons.

2. EXPERIMENTAL SETUP

Two schemes to realize an optical discrete array of waveguides have been proposed. One is a circular multicore optical fiber in which each of the cores supports one mode.²⁷ The cores are relatively close to each other such that their modes overlap, and therefore their energy is coupled. The expected advantage of this realization is the option to have relatively long samples, and therefore weak effects can become significant. However, the fabrication of such multicore samples presents many technological challenges, and solitons in such structures have not been realized to date. Our experiments were carried out in arrays of ridge waveguides.²⁸ A schematic drawing of the sample is shown in the inset of Fig. 2. The array is made from an AlGaAs planar waveguide composed of three layers: an 18% aluminum-doped core, 1.5 μm thick, sandwiched between two layers of 24% doped clad-

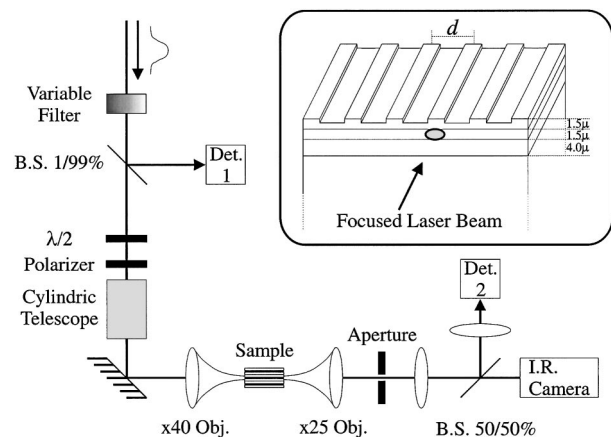


Fig. 2. Experimental setup. Inset: Schematic drawing of the sample. The sample consists of a $\text{Al}_{0.18}\text{Ga}_{0.82}\text{As}$ core layer and $\text{Al}_{0.24}\text{Ga}_{0.76}\text{As}$ cladding layers grown on top of a GaAs substrate. A few samples with different separations d between the waveguides were tested.

ding on top of a GaAs substrate. The upper cladding was $1.5\ \mu\text{m}$ thick, and the lower cladding was $4\ \mu\text{m}$ thick. This slab waveguide was etched to a depth of $0.9\ \mu\text{m}$ through a mask. The etched area of the slab has a lower effective refractive index, and a set of one-dimensional linear waveguides is formed. We choose to work with $4\text{-}\mu\text{m}$ -wide waveguides that support only a single guided mode with an ellipticity ratio of approximately 2:5. We have fabricated array samples with separations between the waveguide centers of $d = 8, 9, 10,$ and $11\ \mu\text{m}$ to check different coupling constants C [see Eq. (1)]. All the arrays are $6\ \text{mm}$ long and contain 41 waveguides. The coupling lengths in all samples are of the order of $1\ \text{mm}$ or longer; hence they are consistent with the weak-coupling assumption that is implied in the coupled-mode theory analysis.

The setup that we used in our experiment is sketched in Fig. 2. A $\times 40$ objective injects the light into the array, and a $\times 25$ objective collects it from the other facet of the sample. Before the beam is launched into the array, it passes a variable filter that controls its power, a set of half-wave plates and polarizers that changes its polarization plane, and a cylindrical telescope. The telescope reshapes the beam profile to match the waveguide mode for a narrow, single-waveguide excitation. When a broader excitation spanning a few waveguides is needed, the telescope is modified accordingly. To measure the input power, we split a portion of the beam off to a calibrated detector. The output facet was imaged onto an infrared camera, and the total transmitted power was measured by another detector. Light from different parts of the output facet could be redirected to an autocorrelator and to a spectrum analyzer in order to measure temporal effects.

Our light source is a commercially available optical parametric oscillator (OPAL), pumped by a 810-nm Ti:sapphire (Tsunami). Pulses of 4 nJ are produced at a repetition rate of 80 MHz. The average power was 300 mW, and each had a peak power of approximately 40 kW. The pulse length was around 100 fs, and the wavelength was tunable between 1450 and 1570 nm. We usually worked at a wavelength of 1530 nm to minimize both two- and three-photon absorption.

In the experiments we measured the distribution of light at the output facet of the sample as we changed various parameters, such as the input power, polarization, initial beam widths, and shapes. We also measured samples with different coupling strengths.

3. BASIC OBSERVATIONS

We start by describing the formation of a discrete spatial soliton from a narrow input. We used an array of $4\text{-}\mu\text{m}$ -wide waveguides with center-to-center separation of $8\ \mu\text{m}$. Light was injected into a single central waveguide. In Fig. 3 we show the output-facet images as captured by the camera for three values of input power. At low power, a wide distribution is observed, spanning approximately 35 waveguides. This distribution fits the expected broadening in a sample 4.2 coupling lengths long (see Fig. 1). When the power is increased, we first observe the light converging toward the input waveguide.

Further increasing the power leads to the formation of a tightly confined distribution around the input waveguide, i.e., a discrete soliton.

Transverse cross sections of the output profile for two samples of different coupling lengths are compared in Fig. 4. Figures 4(a) and 4(b) are from a sample 1.9 coupling lengths long at low and high powers, respectively. Figures 4(c) and 4(d) are from a sample 3.0 coupling lengths long at low and high powers, respectively. The difference in the coupling lengths is due to the different distance between adjacent waveguides in the two samples (11 and $9\ \mu\text{m}$, respectively). The solid curves correspond to the experimentally measured profiles, and the height of the vertical lines represents the calculated light intensity in each waveguide according to a numerical solution of the discrete nonlinear Schrödinger equation [Eq. (1)]. The agreement between the experiment and the numerical solution is good, both at low and at high powers. At low power, most of the light energy is carried by the two outside lobes, while characteristic secondary narrow peaks appear in between. The number of these secondary peaks is an indicator of the total distance in terms of coupling lengths. Both TE and TM polarizations were used in our experiments. Nevertheless, the difference in the coupling coefficients and nonlinear behavior between these polarization states were negligible.

It is interesting to check the power dependence of the visibility of the adjacent peaks in Figs. 3 and 4. The ability to resolve individual waveguide modes in the output distribution depends on the relative phase between them. When the modes of adjacent waveguides are in phase, they are difficult to resolve; when they are completely out of phase, the light intensity dips between them, so that the visibility is increased. Checking the experimental results of Figs. 3 and 4, we observe good visibility for all the low-power results. This is in a good agreement with the $\pi/2$ phase relation predicted by the solution of the linear discrete propagation equation [Eq. (2)]. When the power is increased, the soliton formation forces a smoother phase relation between light in neighboring waveguides, and the mode visibility degrades.

In Figs. 5(a)–5(c) we present the evolution of the output profiles for the two cases of Fig. 4 and for the case of Fig.

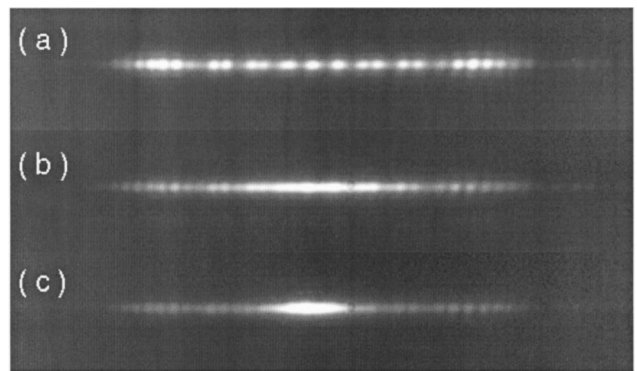


Fig. 3. Images of the output facet of a sample with $d = 4\ \mu\text{m}$ for different powers. (a) Peak power, 70 W. Linear features are demonstrated: two main lobes and a few secondary peaks in between. (b) Peak power, 320 W. Intermediate power, the distribution is narrowing. (c) Peak power, 500 W. A discrete soliton is formed.

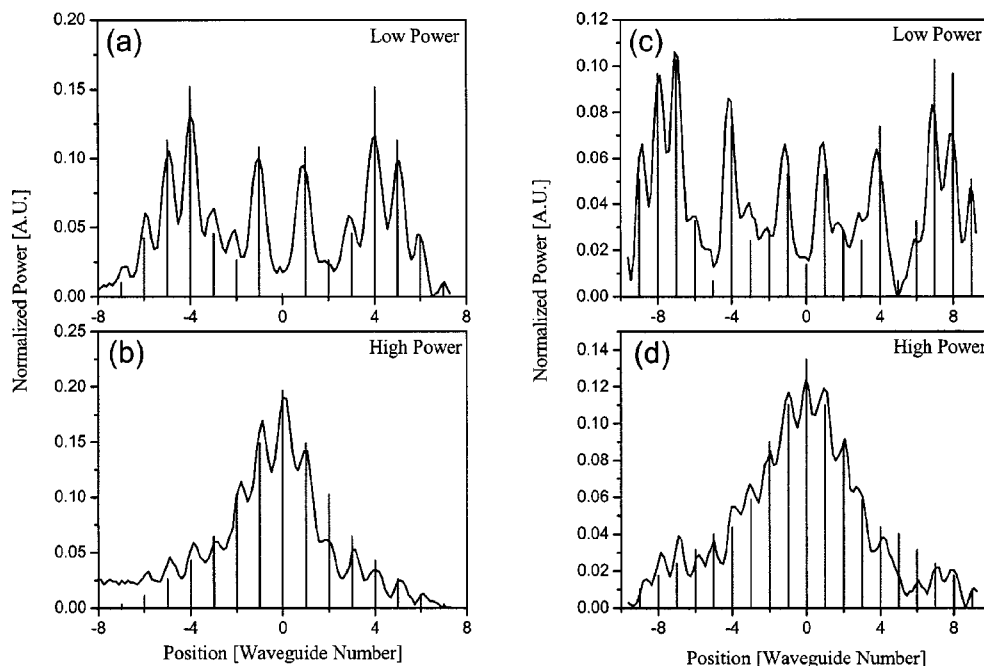


Fig. 4. Single waveguide excitation: experimental and numerical results for samples with $d = 7 \mu\text{m}$ [(a) and (b) total propagation distance of 1.9 coupling lengths] and $5 \mu\text{m}$ [(c) and (d) total propagation distance of 3.0 coupling lengths]. Experimental results are represented by a solid curve, and numerical results are shown as vertical lines. The integrated power is normalized to unity.

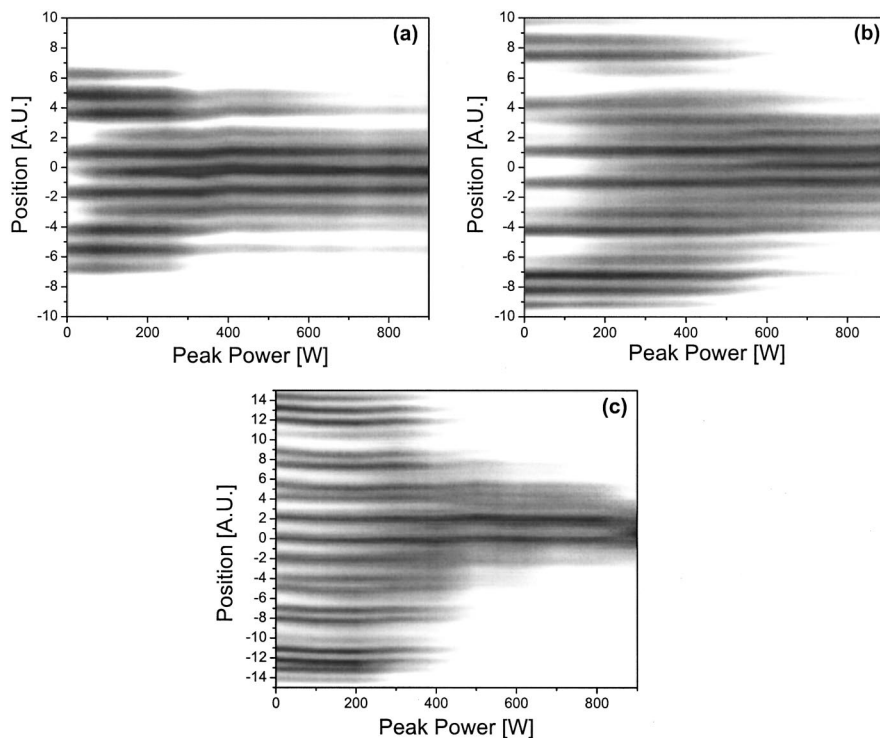


Fig. 5. Single waveguide excitation: output light distributions as a function of the input peak power. Vertical cross sections are the different power profiles corresponding to each input power. (a), (b), and (c) Samples of 1.9, 3.0, and 4.2 coupling lengths, respectively.

3 as a function of input power. Each vertical slice is a cross section of the output distribution at that respective input power. At low power, the light distribution is broad, and, as shown before, most of the light has diffracted away from the input waveguide. As the power is

increased, light is gradually confined to the center of the array. The important fact to note is that, after achieving a certain distribution width, the focusing process arrests, and only a slight variation of the width with power is observed.

4. FORMATION OF DISCRETE SOLITONS FROM VARIOUS EXCITATIONS

Until now, we have described only discrete solitons that were formed by the launching of light into a single central waveguide. This is equivalent to exciting uniformly all available spatial frequencies because a single waveguide represents a discrete delta-function excitation. The single-waveguide excitation is the case in which the discrete nature of the waveguide array is most pronounced. As discussed in Ref. 29, the continuous and discrete diffraction curves have the same curvature for small spatial frequencies. Only when high-enough frequencies are excited in the array is discreteness relevant.

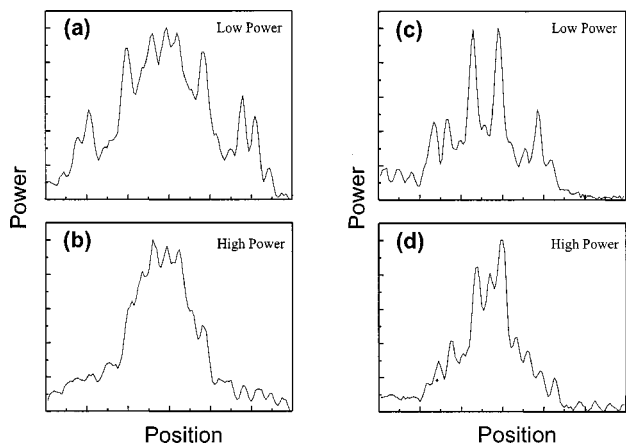


Fig. 6. Wide excitation by power splitting: output profiles of (a) and (b) three-waveguide-wide (c) and (d) five-waveguide-wide excitations. All the samples are of 3.0 coupling lengths.

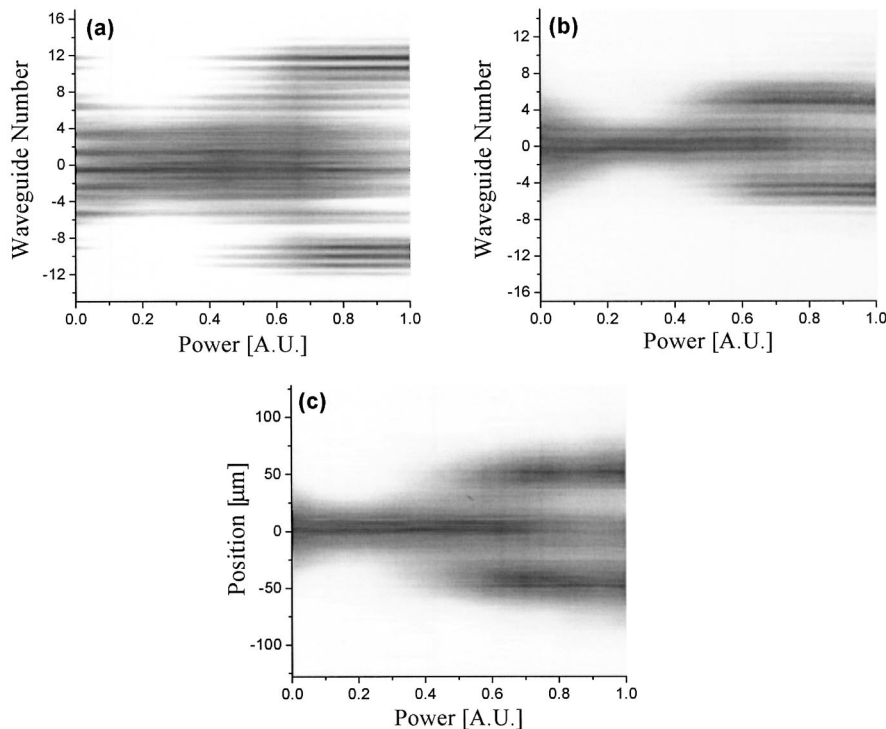


Fig. 7. Wide excitation by a wide smooth beam: output light distributions as a function of the input peak power as in Fig. 5. (a) A two-waveguide-wide excitation. (b) A three-waveguide-wide excitation. (c) A three-waveguide-wide excitation of a continuous slab waveguide.

Solitons that span a few waveguides are very similar to their counterparts in a continuous slab waveguide. Only very narrow solitons are expected to show unique features that stem from discreteness.

To excite wider solitons, we used arrays with power splitters as input channels. The power splitters were multiple junctions, which split the launched power from one input waveguide almost equally into several waveguides. The even splitting was verified experimentally in a different sample. The output of the splitter was injected into the waveguide array such that each splitter branch is coupled into one waveguide. As a result, the launched light distribution is a discrete rectangular function. It is narrower in its frequencies content, but, owing to the sharp distribution edges, it still contains all the high spatial frequencies.

Figure 6 presents the results for low and high power when the power was split into three and five waveguides. The output profiles for a three-waveguide input are plotted on Figs. 6(a) and 6(b) and for a five-waveguide input on Figs. 6(c) and 6(d). The array spacing is $9 \mu\text{m}$ for both samples, corresponding to 3.0-coupling-length propagation. In the linear, low-power cases, we observe a lower degree of diffraction compared with single-waveguide excitation in which light expanded over approximately 20 waveguides. In the case in which three and five input waveguides were excited, the output expands over 17 and 11 waveguides, respectively. We also observe the usual features of discreteness: power concentration at the distribution edges and a few peaks in between. Increasing the power causes both distributions to become smoother and narrower. The nonlinearity causes the phases to lock together, and the mode visibility is degraded.

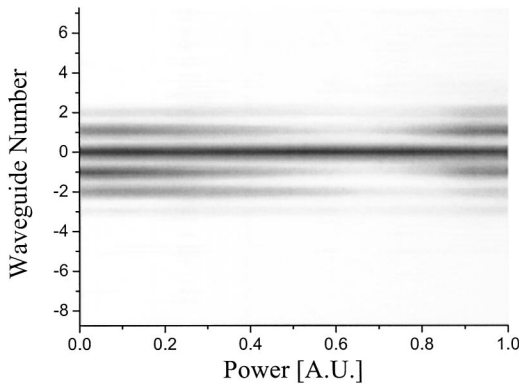


Fig. 8. Nonlinear contraction of power into a single waveguide.

There is an alternative way to launch a broad light distribution with reduced sharp features (hence a narrower band of spatial frequencies). We inject the light directly into the array after shaping the input beam as a wide ellipse through cylindrical optics. The beam width overlaps a few waveguides, exciting them according to the beam-intensity profile. Even though the input beam excites the region between the waveguides also, it can be shown that most of the energy is coupled into the waveguides; this excitation corresponds to the fundamental band of the periodic structure, which is described by the coupled-mode theory. Higher-order modes of the structure, which correspond to light trapped between the waveguides, are also excited but with significantly lower efficiency. The results of two such experiments are presented in Fig. 7. Beams covering approximately two and three waveguides were launched, and their output profiles as a function of input power are shown in Figs. 7(a) and 7(b), respectively. As before, we observe the formation of discrete solitons. Nevertheless, they now behave much like regular continuous solitons as their profile is bell shaped and only their width changes as the power is increased. As with continuous one-dimensional solitons, less power is required to form a wider soliton; therefore the minimal width is reached at weaker intensities as compared with the single-waveguide input case.

As the power is increased so that there is enough power for two solitary beams, the discrete soliton splits instead of becoming narrower. This result has been observed with the continuous spatial solitons and explained as an instability of the second soliton. The cause for this instability is probably a perturbation to the soliton shape by two-photon absorption.³⁰ The splitting of a three-waveguide-wide discrete soliton and of a continuous soliton in a planar slab waveguide are compared in Figs. 7(b) and 7(c), respectively. The two results are strikingly similar, confirming that with this wide excitation discrete optics can be described by the continuous limit. Recalling that a single waveguide excites all the frequencies of the Brillouin zone between $-\pi$ and π , it follows that a two-waveguide input would excite approximately half of this range ($-\pi/2$ to $\pi/2$), in which the diffraction curve has only one curvature, much like a semicircle. It should not be surprising then that a three-waveguide beam, which excites an even narrower range of spatial frequencies ($-\pi/3$ to $\pi/3$), behaves much like in a continuum.

Using specific conditions of wide excitation and very weak coupling between the waveguides, we were able to confine most of the light into a single central waveguide. The output distribution as a function of input power is depicted in Fig. 8. When the power is increased, the distribution narrows until all the light is guided into a single waveguide. Further increase of the power causes the light to couple back into more waveguides. Such behavior is explained by nonlinear two-photon attenuation, which is enhanced at the large intensity achieved when the power is concentrated in one waveguide.

In all the experiments described above, the main reason for differences between the results and the predictions of coupled-mode theory is the pulse temporal evolution. With coupled-mode theory there is an underlying assumption of a cw excitation. To investigate the temporal behavior, we recorded autocorrelation traces of a discrete soliton. A slit was used to select light either from the soliton center or from its wing, a few waveguides away from the input center. The two traces, together with the input pulse autocorrelation, are shown in Fig. 9(a). The pulse length at the soliton center is doubled owing to the normal dispersion of AlGaAs and the nonlinear effect of self-phase modulation. At the soliton wing, there is evidence for temporal splitting. This splitting is due to the depletion of light from the wing near the temporal center of the pulse because of a stronger spatial focusing. To illustrate this behavior, we draw a spatial-temporal profile of the pulse in Fig. 9(b). The spectral broadening in the central waveguide, shown in Fig. 9(c), illustrates the importance of self-phase modulation to the temporal evolution. We can estimate from the oscillatory profile of the output spectrum that self-phase modulation introduces a nonlinear phase shift of approximately $3\pi/2$.

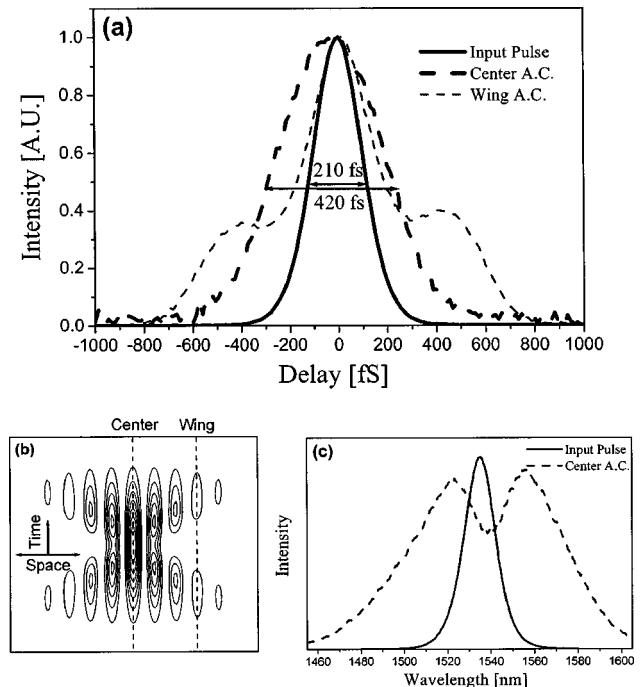


Fig. 9. (a) Temporal autocorrelations of a discrete soliton: the input pulse (solid curve), the output pulse center (thick dashed curve), and the output pulse wing (thin dashed curve). (b) The output pulse sketch. (c) A comparison between the spectra of the input (solid curve) and the output (dashed curve) pulses.

5. CONCLUSIONS

We presented the results of experiments investigating the formation of optical discrete solitons. They were demonstrated with different input conditions, spanning the range between strong discreteness to quasi-continuity. Results are interpreted within the framework of coupled-mode theory and verified with good agreement. The temporal evolution of the light pulses in our samples was also studied to understand its effect. For low power and a narrow excitation width, the beam expands according to discrete diffraction, in which energy is transported mainly on the wings. For wider excitations, discrete and continuous diffractions become more and more similar. When the input power is increased, a discrete soliton is formed in all cases. Higher energies are required to form solitons from a narrow input. For the same power levels, when the input beam is broad (two or more waveguides excited), soliton splitting is observed. Such splitting is caused by the presence of nonlinear absorption in the material.

The combination of normal dispersion and focusing nonlinearity causes temporal broadening of the pulse while propagating in the waveguide. In particular, self-focusing takes place mainly in the central portion of the beam. Temporal pulse splitting is observed in the wings of the spatial distribution. All these features lead to a combination of novel effects, which may be exploited in future all-optical interconnect and switching applications.

ACKNOWLEDGMENTS

The authors thank D. N. Christodoulides, D. Modotto, and M. Sorel for different contributions to this paper. We also acknowledge the Engineering and Physical Sciences Research Council in the United Kingdom and the Ministry of Science and Technology in Israel for financial support to this project.

Y. Silberberg can be reached by e-mail at yaron.silberberg@weizmann.ac.il.

*Also with the Department of Electronics and Electrical Engineering, University of Glasgow, Glasgow, Scotland, G12 8QQ.

REFERENCES

- V. E. Zakharov and A. B. Shabat, "Exact theory of two-dimensional self-focusing and one-dimensional self-modulation of waves in nonlinear media," *Zh. Eksp. Teor. Fiz.* **61**, 118–134 (1971) [*Sov. Phys. JEPT* **34**, 62–69 (1972)].
- L. F. Mollenauer, R. H. Stolen, and J. P. Gordon, "Experimental observation of picosecond pulse narrowing and solitons in optical fibers," *Phys. Rev. Lett.* **45**, 1095–1098 (1980).
- A. Barthelemy, S. Maneuf, and C. Froehly, "Propagation soliton et auto-confinement de faisceaux laser par non linearite' optique de Kerr," *Opt. Commun.* **55**, 201–206 (1985).
- J. S. Aitchison, A. M. Weiner, Y. Silberberg, M. K. Oliver, J. L. Jackel, D. E. Leaird, E. M. Vogel, and P. W. E. Smith, "Observation of spatial optical solitons in a nonlinear glass waveguide," *Opt. Lett.* **15**, 471–473 (1990).
- W. E. Torruellas, Z. Wang, D. J. Hagan, E. W. VanStryland, G. I. Stegeman, L. Torner, and C. R. Menyuk, "Observation of 2-dimensional spatial solitary waves in a quadratic medium," *Phys. Rev. Lett.* **74**, 5036–5039 (1995).
- M. Segev, B. Crosignani, A. Yariv, and B. Fischer, "Spatial solitons in photorefractive media," *Phys. Rev. Lett.* **68**, 923–926 (1992).
- G. C. Duree, J. L. Shultz, G. J. Salamo, M. Segev, A. Yariv, B. Crosignani, P. Di Porto, E. J. Sharp, and R. R. Neurgaonkar, "Observation of self-trapping of an optical beam due to the photorefractive effect," *Phys. Rev. Lett.* **71**, 533–536 (1993).
- D. N. Christodoulides and R. I. Joseph, "Discrete self-focusing in nonlinear arrays of coupled waveguides," *Opt. Lett.* **13**, 794–796 (1988).
- H. S. Eisenberg, Y. Silberberg, R. Morandotti, A. R. Boyd, and J. S. Aitchison, "Discrete spatial optical solitons in waveguide arrays," *Phys. Rev. Lett.* **81**, 3383–3386 (1998).
- A. S. Davydov, "Solitons in molecular systems," *Phys. Scr.* **20**, 387–394 (1979).
- T. Holstein, "Studies of polaron motion," *Ann. Phys. (N.Y.)* **8**, 325–289 (1959).
- P. Marquié, J. M. Bilbault, and M. Remoissenet, "Observation of nonlinear localized modes in an electrical lattice," *Phys. Rev. E* **51**, 6127–6133 (1995).
- B. Denardo, B. Galvin, A. Greenfield, A. Larranza, S. Putterman, and W. Wright, "Observations of localized structures in nonlinear lattices: domain walls and kinks," *Phys. Rev. Lett.* **68**, 1730–1733 (1992).
- S. Flach and C. R. Willis, "Discrete breathers," *Phys. Rep.* **295**, 182–264 (1998).
- A. L. Jones, "Coupling of optical fibers and scattering in fibers," *J. Opt. Soc. Am.* **55**, 261–271 (1965).
- A. C. Scott and L. Macneil, "Binding energy versus nonlinearity for a 'small' stationary soliton," *Phys. Lett. A* **98**, 87–89 (1983).
- A. B. Aceves, C. De Angelis, T. Peschel, R. Muschall, F. Lederer, S. Trillo, and S. Wabnitz, "Discrete self-trapping, soliton interactions, and beam steering in nonlinear waveguide arrays," *Phys. Rev. E* **53**, 1172–1189 (1996).
- R. Morandotti, U. Peschel, J. S. Aitchison, H. S. Eisenberg, and Y. Silberberg, "Dynamics of discrete solitons in optical waveguide arrays," *Phys. Rev. Lett.* **83**, 2726–2729 (1999).
- Y. S. Kivshar, W. Królikowski, and O. A. Chubukalo, "Dark solitons in discrete lattices," *Phys. Rev. E* **50**, 5020–5032 (1994).
- S. Darmanyan, A. Kobayakov, E. Schmidt, and F. Lederer, "Strongly localized vectorial modes in nonlinear waveguide arrays," *Phys. Rev. E* **57**, 3520–3530 (1998).
- Y. S. Kivshar and D. K. Campbell, "Peierls–Nabarro potential barrier for highly localized nonlinear modes," *Phys. Rev. E* **48**, 3077–3081 (1993).
- R. Muschall, C. Schmidt-Hattenberger, and F. Lederer, "Spatially solitary waves in arrays of nonlinear waveguides," *Opt. Lett.* **19**, 323–325 (1994).
- I. Relke, "Instability of solitons in an inhomogeneous array of optical fibers," *Phys. Rev. E* **57**, 6105–6111 (1998).
- W. Królikowski and Y. S. Kivshar, "Soliton-based optical switching in waveguide arrays," *J. Opt. Soc. Am. B* **13**, 876–887 (1996).
- U. Peschel, R. Morandotti, J. S. Aitchison, H. S. Eisenberg, and Y. Silberberg, "Nonlinearly induced escape from a defect state in waveguide arrays," *Appl. Phys. Lett.* **75**, 1348–1350 (1999).
- U. Peschel, R. Morandotti, J. S. Aitchison, H. S. Eisenberg, and Y. Silberberg, "Discrete solitons. II. Dynamical properties," *J. Opt. Soc. Am. B* (to be published).
- C. Schmidt-Hattenberger, U. Trutschel, R. Muschall, and F. Lederer, "Envelope description of an optical fiber array with circularly distributed multiple cores," *Opt. Commun.* **82**, 461–465 (1991).
- P. Millar, J. S. Aitchison, J. U. Kang, G. I. Stegeman, A. Villeneuve, G. T. Kennedy, and W. Sibbett, "Nonlinear waveguide arrays in AlGaAs," *J. Opt. Soc. Am. B* **14**, 3224–3231 (1997).
- H. S. Eisenberg, Y. Silberberg, R. Morandotti, and J. S. Aitchison, "Diffraction management," *Phys. Rev. Lett.* **85**, 1863–1866 (2000).
- Y. Silberberg, "Solitons and 2-photon absorption," *Opt. Lett.* **15**, 1005–1007 (1990).